COMPARATIVE STUDY OF MECHANICAL INHOMOGENEITY OF LASER AND FRICTION STIR WELDED JOINTS OF Al-Mg-Si ALLOY

IVANOV Sergei[1], PANCHENKO Oleg[1], MICHAILOV Vesselin[2], KARKHIN Victor[1], VELICHKO Olga[3]

[1] *Peter the Great St.Petersburg Polytechnic University, St.Petersburg, Russian Federation*
[2] *Brandenburg University of Technology, Cottbus, Germany, EU*
[3] *Laser Technologies Centre, St. Petersburg, Russian Federation*

Abstract

Microstructural and mechanical inhomogeneity of laser beam (LBW) and friction stir (FSW) welded joints of 4 mm thick 6082-T6 Al-Mg-Si alloy was studied. Thermal cycles measured in heat affected zone (HAZ) showed that LBW has a much higher heating and cooling rates than FSW. Distribution of local microhardness and local strain in tensile specimens revealed that fracture of the joints corresponds to a region with minimum hardness. LBW tensile samples were fractured in weld metal, FSW samples - in HAZ. It has been found that tensile properties and ductility of joints is significantly lower than those of the base metal. The LBW and FSW joint efficiency in terms of yield stress was about 71% and 61% respectively. Joint efficiency in terms of elongation was 7.8% (LBW) and 19% (FSW). It is explained by the strain concentration in the lower strength joint region.

Keywords: Friction stir welding, laser welding, Al-Mg-Si alloy, temperature field, microstructure

INTRODUCTION

Wide usage of aluminum alloys in integrated structures are impeded its poor weldability by arc welding. The main defects during arc welding are the pore formation [1, 2], the softening in the heat affected zone (HAZ) [3, 4] and hot cracking [5-7]. Slot welds cannot be obtained by arc welding due to presence of refractory aluminum oxide film on the surface of aluminum alloy. Advanced joining technologies, such as laser beam welding (LBW) and friction stir welding (FSW), allows obtaining high-quality joints. A high energy concentration into the laser beam produces joints with a narrow HAZ. It is important during welding of heat treatable aluminum alloys. The main disadvantages of LBW are low efficiency, pore formation and evaporation of alloying elements [8, 9]. Friction stir welding have no defects associated with the melting of metal, since FSW is the solid state joining technology. Low manufacturability, expensive tooling and a narrow range of joint types greatly limits usage of FSW in production [10].

The nature of welded joint formation during LBW and FSW of Al-Mg-Si alloys is widely described in literature. Most of publications are focused on the origin of defect formation and the effects of welding conditions on it. Data about effects of thermo-deformation welding cycle on distribution of local mechanical properties are limited [11-14].

The aim of the paper is to study the effects of LBW and FSW thermo-deformation cycles on formation of local mechanical properties and strength of welded joints.

1. EXPERIMENTAL PROCEDURE

In this study, investigations were carried using 4 mm thick sheets of 6082-T6 aluminum alloy. Chemical composition of the alloy was 0.7 % Mg, 1.0 % Si, 0.07 % Cu, 0.51 % Mn, 0.08 % Zn, 0.39 % Fe (weight %). T6 heat treatment (combination of quenching following the solution heat treatment) allows obtain the following mechanical properties of the base metal: yield strength 298 MPa, tensile strength 340 MPa, elongation 22 %. Some of T6 sheets were solution heat treated and naturally aged (T4 heat treatment) in order to obtain mechanical properties of alloy in T4 conditions.

Laser beam welding was carried out using Reis RLP 16-TF robotic system equipped with 15 kW fiber laser. Sheets were welded without groove and any filler material. Welding conditions were the following: speed 50 mm/s, beam power 6.3 kW. The FSW trials were carried out using UNITECH 3-axis milling machine. Conical threated pin with diameter 6.5 mm and 18 mm shoulder was used. The FSW conditions were the following: welding speed 4.2 mm/s, rotation rate 1120 rpm, tilt angle 2°.

Thermal cycles were measured using HBM QuantumX MX1609 set-up and K-type thermocouples. Acquisition rate was 5 Hz during FSW and 50 Hz during LBW.

The specimens for microstructure analysis were etched in Keller's reagent (2 ml HF, 3 ml HCl, 5 ml HNO_3, 190 ml H_2O) [15]. The microstructure was examined using the LEICA DMI5000M light metallographic microscope with magnification up to 1000. Hardness was measured using Wilson Wolpert 452SVD Vickers hardness tester with diamond pyramid indenter under load of 5 N according to ISO 6507. Energy dispersive X-ray (EDX) analysis and fractography was conducted by the use of Zeiss Supra 40VP scanning electron microscope with Oxford Instruments Inca X-Act EDX spectrometer.

The tensile properties were tested by using transverse tensile specimens of a 4x20 mm rectangular cross-section in accordance with the Russian standard GOST 1497-84 (type 1, number 22) (**Figure 1**). Tensile test were carried out at room temperature on a hydraulic universal testing machine Super L 60 (Tinius Olsen) at the testing speed of 0.07 mm/s. To determine strain distribution in the weld, transverse lines with spacing of 0.5 mm were laser marked on the face side of the weld specimen prior the tensile test. After the tensile test, each length between the lines was measured by optical microscopy and the strains were calculated.

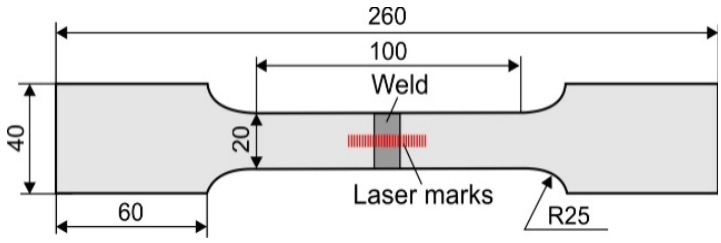

Figure 1 Tensile specimen configuration

2. MICROSCTRUCTURE

The main difference between studied welding technologies is the nature of joint formation. Local melting of welded materials during LBW leads to formation of the weld bead with as-cast microstructure (**Figure 2**). During FSW material is heated by the friction and plastic deformation up to nearly solidus temperature [16]. Microstructure of FSW joint weld metal consists of grains after dynamic recrystallization. The recrystallized region is often called the "nugget", which is a descriptive term, though not very scientific. Terms such as "dynamically recrystallized region (DRR)" have been suggested and used extensively in the literature [17].

As-cast microstructure of LBW weld metal consisted of dendrites growing from the fusion line in the direction of change of the temperature gradient during solidification of molten pool and equiaxed grains near the weld centerline (**Figure 2**). Formation of equiaxed grains is explained in the following way: as the heat input and the welding speed are increased, the temperature gradient (G) at the end of the tear-shaped weld pool is reduced and consequently the constitutional supercooling at the centerline is increased [18, 19]. Equiaxed grains form a band along the centerline of the weld and block off columnar grains and prevent formation of layer of liquid metal at the centerline. It sufficiently reduces susceptibility to hot cracking during welding [20]. Any microstructure changes in HAZ cannot be observed using optical microscopy. Boundaries and transition of HAZ can be determined by the microhardness measurements.

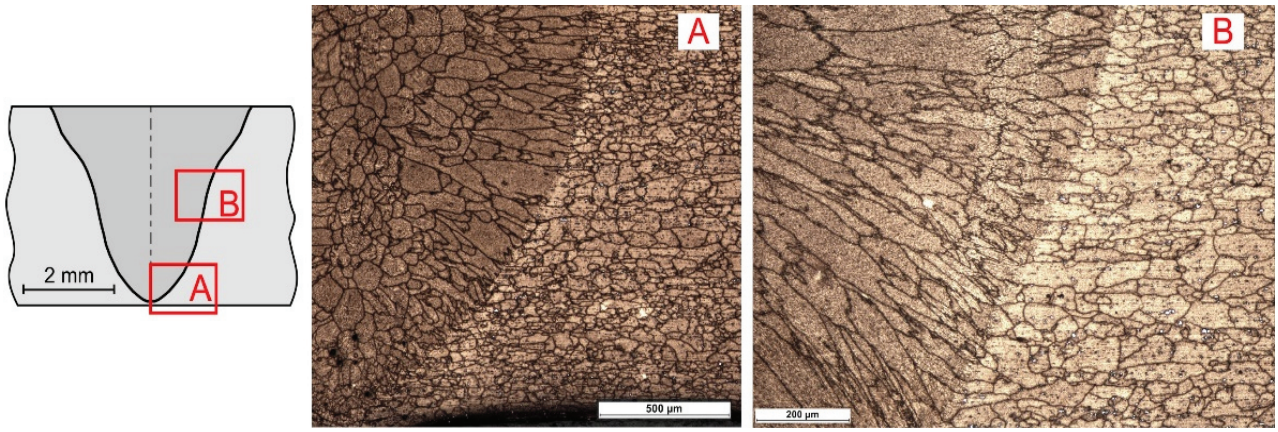

Figure 2 Schematic cross section and microstructure of laser beam welded joint

Microstructure of DDR of FSW joint consisted of fine-grained microstructure (**Figure 3**). Equiaxed grains were in 20 times smaller than those of base metal. Sufficient plastic deformation during FSW allied with high heating temperature leads to breaking up the grains, growth and dissolution of β'' particles, redistribution of dislocation and changing its density [21]. Thermo-mechanically affected zone (TMAZ) was revealed between DDR and HAZ. The microstructure of TMAZ consisted of a mixture of recrystilized and polygonised grains. Grains with visible subgrain microstructure were revealed in the TMAZ.

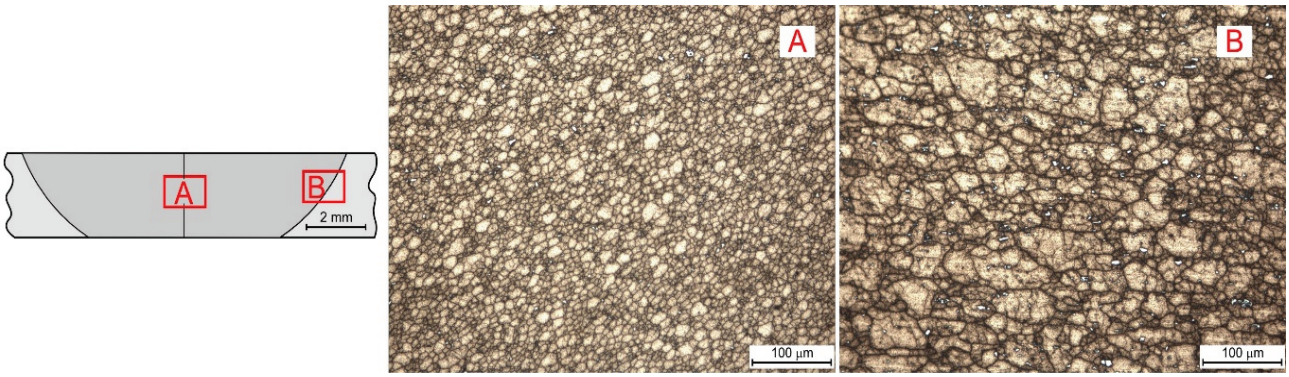

Figure 3 Schematic cross section and microstructure of friction stir welded joint

3. THERMAL CYCLES DURING WELDING

It is known that mechanical properties of heat treatable aluminum alloys completely depend on size, morphology and distribution of dispersed particles [3, 4, 11, 21]. Origin, growth and dissolution of particles are controlled by the rate of thermo-diffusional processes. Diffusion in HAZ of welded joint depends on the temperature field during welding. The following two parameters describe temperature field in current point: peak temperature and heating/cooling rate or dwell time in temperature range.

Temperature field during welding depends on the spatial distribution of energy in the heat source and effective heat input. Analysis of thermal cycles (**Figure 4a**) showed that heating time from ambient temperature to the peak temperature was in 18 times higher during LBW then during FSW, cooling time from peak temperature to the 100 °C was in 2 times lower during LBW. It indicates that HAZ exposes in high temperature rage much longer during FSW.

During FSW peak temperature on the top surface of the sheets reached 509 °C on advancing side (**Figure 4b**). Asymmetry of temperature field in FSW joint was revealed. It can be explained by the more intensive plastic

deformation of metal on advancing side then on retreating side. This statement is in agreement with the experimental measurement of temperature field in FSW tool during welding [22]. Peak temperature during LBW reaches liquidus at the fusion line. High temperature gradient in cross section of LBW joint and high heating/cooling rate helps to form narrow HAZ with dramatic change of properties.

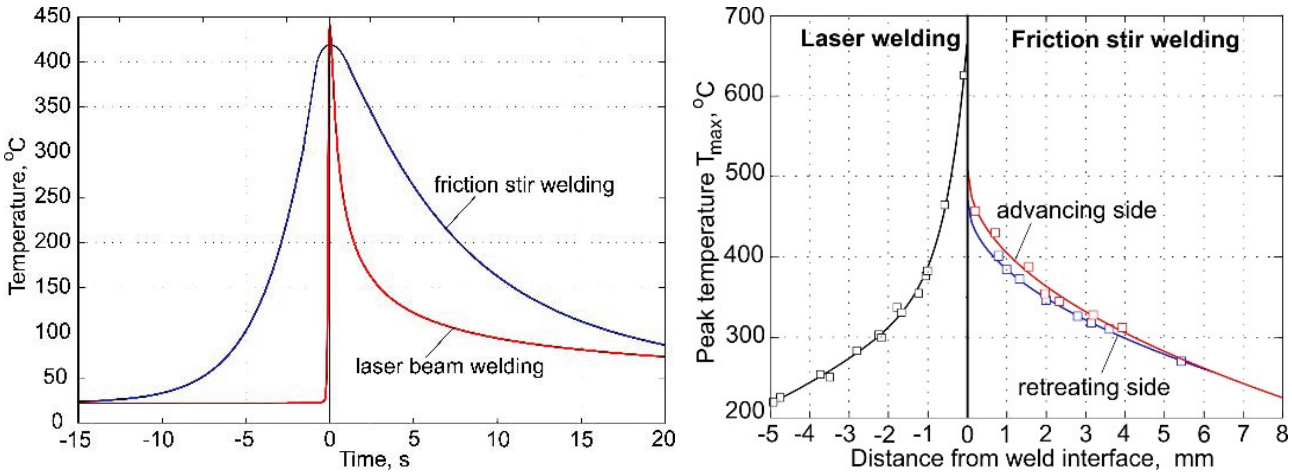

a) b)

Figure 4 Thermal cycles (a) and peak temperature distribution (b) in HAZ during FSW and LBW

4. MECHANICAL PROPERTIES

Metal heating higher than 260 °C during LBW led to hardness reduction (**Figures 4, 5**). Overaging of metal at 1.5 mm distance corresponded to the peak temperature range 260-320 °C led to dramatic hardness drop in 30% from 112.5 HV (T6 base metal) to 88 HV. Further heating up to liquid temperature did not cause sufficient hardness change due to partial dissolution of β'' particles, as conformed that hardness is higher than T4 metal hardness. Minimal joint hardness of 73.5 HV corresponded to the weld metal with as-cast microstructure.

Reduction of hardness in HAZ of FSW joint was revealed in 10 mm long region which in 2.9 times longer than during LBW. Asymmetry of hardness profiles owing to higher heat generation on advancing side was detected. Lower hardness corresponded to higher peak temperature. General tendency was the reduction of hardness in HAZ down to 67.4-69.4 HV during rising of temperature to 350 °C. Hardness decrease lower then T4 metal indicates formation of coarse β' and β particles and reduction of density of β'' particles. Hardness was raised at 1.65-1.80 mm distance from weld interface corresponded to the peak temperature range 350-450 °C. It is explained by the natural aging following by the total dissolution of Mg_2Si particles during welding.

Analysis of peak temperature distributions and microhardness profiles revealed that at the same peak temperature hardness of FSW joint is lower than LBW joint. At 350 °C hardness of FSW joint was 20 % lower than LBW due to sufficient lower heating and cooling rates during FSW.

Table 1 Mechanical properties of welded joints

	T6 metal (base metal)	FSW joint	LBW joint	T4 metal
Yield stress (MPa)	298	181	213	149
Tensile stress (MPa)	340	245	227	260
Elongation (%)	22	4.2	1.7	28

Morphology and local distribution of dispersed Mg_2Si particles determines the microhardness and strength of welded joint. Tensile tests revealed that LBW and FSW joint have similar level of mechanical properties (**Table 1**). Joint efficiency in terms of yield stress was 72% for FSW and 67 % for LBW. Elongation of FSW welded joint was in 5.3 time lower then base metal, LBW joint was in 12.3 time lower. Significant loses in ductility are explained by the strain concentration in the lower strength weld region, as expected from the hardness profile of the joint (**Figure 5**).

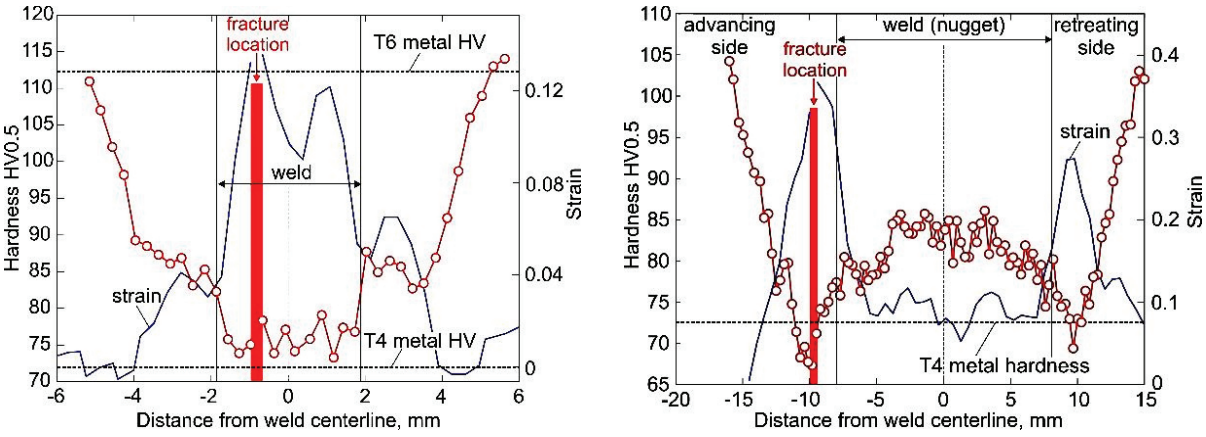

a) b)

Figure 5 Microhardness profile in HAZ and distribution of residual plastic strain in tensile specimen of FSW (a) and LBW (b) welded joints

5. CONCLUSION

1) Laser and friction stir welded joints have pronounced inhomogeneity of microstructure and mechanical properties in HAZ.
2) Asymmetry of peak temperature field and microhardness distribution is revealed in FSW joint.
3) Joint efficiency in terms of yield stress is 72% for FSW and 67% for LBW. Elongation of FSW welded joint is in 5.3 time lower than that of the base metal, LBW joint is in 12.3 time lower.
4) Distribution of local microhardness and local strain in tensile specimens revealed that fracture of the joints corresponds to the region with minimal hardness. LBW tensile samples were fractured in weld metal, FSW samples - in HAZ.
5) At the same peak temperature hardness of FSW joint is lower than LBW joint due to sufficient lower heating and cooling rates during FSW.

ACKNOWLEDGEMENTS

The research has been performed at the Peter the Great St. Petersburg Polytechnic University under the contract № 14.Z50.31.0018 with the Ministry of Education and Science of the Russian Federation)

REFERENCES

[1] TREVISAN, R. E., SCHWEMMER, D. D., OLSON, D. L. *The Fundamental of Weld Metal Pore Formation*. Welding: Theory and Practice, Chap. 3, Elsevier Science Pub. 1990.

[2] SHORE, R. J., MCCAULEY, R. B. Effect of porosity on high strength aluminum 7039. *Welding Journal*, 1970, vol. 49, no. 7, pp. 311-321.

[3] MHYR, O. R., GRONG, O. Process modelling applied to 6082-T6 aluminum weldments I. Reaction Kinetics. *Acta Materialia*, 1991, vol. 39, pp. 2693-2702.

[4] GRONG, O. *Metallurgical Modelling of Welding*. Inst. of Metals Pub., London, 1997.

[5] MARTIKAINEN, J., HILTUNEN, E., KARKHIN, V. A., IVANOV, S. Y. A method for evaluating the liquation cracking susceptibility of welded joints in Al-Mg-Si alloys. *Welding International*, 2013, no. 2, pp. 139-143.

[6] HUANG, C., KOU, S. Liquation cracking in full-penetration Al-Mg-Si welds. *Welding Journal*, 2004, vol. 83, no. 4, pp. 111-122.

[7] CHANG, C. C. Microstructure in hot cracking mechanism of welded aluminium alloys. *Materials Science and Technology*, 2013, vol. 29, no. 4, pp. 504-510.

[8] KATAYAMA, S. *Handbook of Laser Welding Technologies*. Woodhead Publishing. 2013, 654 p.

[9] DILTHEY, U., GOUMENIOUK, A., LOPOTA, V., TURICHIN, G., VALDAITSEVA, E. Development of a theory for alloying element losses during laser beam welding. *Journal of Physics D: Applied Physics*, 2001, vol. 34, no. 1, pp. 81-86.

[10] KALLEE, S. W. Industrial Applications in Friction Stir Welding. D. Lohwasser and Z. Chen (eds). Friction stir welding. From basic to applications. Cambridge: Woodhead Publishing, 2010, pp. 118-163.

[11] GALLAIS, C., SIMAR, A., FABREGUE, D., DENQUIN, A., LAPASSET ,G., DE MEESTER, B., BRECHET, Y., PARDOEN, T. Multiscale analysis of the strength and ductility of aa 6056 aluminum friction stir welds. *Metallurgical and Materials Transactions*. 2007, vol. 38A, pp. 964-981.

[12] WEIS OLEA, C. A. Influence of energy input in friction stir welding on structure evolution and mechanical behaviour of precipitation-hardening in aluminium alloys (AA2024-T351, AA6013-T6 and Al-Mg-Sc). GKSS-Forschungszentrum Geesthacht GmbH. 2008.

[13] MORITA, T., YAMANAKA, M. Microstructural evolution and mechanical properties of friction-stir-welded Al-Mg-Si joint. *Materials Science and Engineering: A*. 2014, vol. 595, no. 10, pp. 196-204.

[14] VELICHKO, O. V., IVANOV, S. YU., KARKHIN, V. A., LOPOTA, V. A., MAKHIN, I. D. Friction stir welding of thick plates of Al-Mg-Sc alloy. *Welding International*. 2016, vol. 30, no. 8, pp. 630-634.

[15] *ASM Handbook: Vol. 9: Metallography and Microstructures*. ASM International, Materials Park, Ohio, USA, 2004. 1184 p.

[16] UPADHYAY, P., REYNOLDS, A. Effect of backing plate thermal property on friction stir welding of 25 -mm-thick AA6061. *Metallurgical and Materials Transactions A,* 2014, vol. 45, pp. 2091-2100.

[17] THREADGILL, P. L., LEONARD, A. J., SHERCLIFF, H. R., WITHERS, P. J. Friction stir welding of aluminium alloys. *International Materials Reviews*, 2009, vol. 54, no. 2, pp. 49-93.

[18] KARKHIN, V. A., ILIN, A. S., PESEN, H. J., PRIKHODOVSKY, A. A., PLOCHIKHINE, V. V., MAKHUTIN, M. V., ZOCH, H.-W. Effects of latent heat of fusion on thermal processes in laser welding of aluminium alloys. *Science and Technology of Welding and Joining*, 2005, vol. 10, no. 5, pp. 597-603.

[19] RAYAMYAKI, P., KARKHIN, V.A., KHOMICH, P.N. Determination of the main characteristics of the temperature field for the evaluation of the type of solidification of weld metal in fusion welding. *Welding International*, 2007, vol. 21, no. 7, pp. 600-604.

[20] PLOSHIKHIN, V., PRIKHODOVSKY, A., MAKHUTIN, M., ILIN, A., ZOCH H.-W. *Integrated mechanical-metallurgical approach to modeling of solidification cracking in welds. Hot Cracking Phenomena in Welds*. T. Boellinghaus, and H. Herold (eds). Springer. 2005, pp. 223-244.

[21] SATO, Y. S., URATA, M., KOKAWA, H. Parameters controlling microstructure and hardness during friction-stir welding of precipitation-hardenable aluminum alloy 6063. *Metallurgical and Materials Transactions A*, 2002, vol. 33, no. 3, pp. 625-635.

[22] FEHRENBACHER, A., DUFFIE, N. A., FERRIER, N. J., ZINN, M. R., PFEFFERKORN, F. E. Temperature measurement and closed-loop control in friction stir welding. In *8th International Friction Stir Welding Symposium*, Timmendorfer Strand, Germany, 2010, 19 p.